



Analyses of direct verification data of Rockwell diamond indenters by iterative regression method

Satoshi Takagi

National Metrology Institute of Japan, AIST, AIST Tsukuba Central 3, 1-1-1, Umezono, Tsukuba 305-8563 Japan

ABSTRACT

For the verification of Rockwell diamond indenters exactly compliant to the international definition, an iterative method with the least square circle fitting was introduced. This method was applied to the analysis of verification data obtained with a laser probe 3D profile measurement instrument. The geometry of a Rockwell diamond indenter was verified with the equipment as an example. Conventional analyses on cross sections of an indenter is demonstrated as well as three dimensional analysis of indenter geometry. The analyses on cross sections showed that the technique can be used to express the geometrical parameters described in the definition of CIPM/CCM/WGH properly, whereas three dimensional analysis enables to express the imperfection of geometry with fewer parameters. In addition, this technique can be applicable to determine equivalent geometrical parameters obtained with the optical measurement system currently used at the National Metrology Institute of Japan (NMIJ) to establish the national standard indenters. It is shown that the proposed method describes the geometry of indenter better than currently used method. These results suggest that the uncertainty of the national standard indenter could be improved through this high resolution geometry measurement and the multiple regression analysis NMIJ is using.

Section: RESEARCH PAPER

Keywords: Rockwell diamond indenter; tip radius; cone angle; laser probe 3D profile measurement instrument; least square circle fitting

Citation: Satoshi Takagi, Analyses of direct verification data of Rockwell diamond indenters by iterative regression method, Acta IMEKO, vol. 3, no. 3, article 5, September 2014, identifier: IMEKO-ACTA-03 (2014)-03-05

Editor: Paolo Carbone, University of Perugia

Received April 1st, 2013; **In final form** August 20th, 2014; **Published** September 2014

Copyright: © 2014 IMEKO. This is an open-access article distributed under the terms of the Creative Commons Attribution 3.0 License, which permits unrestricted use, distribution, and reproduction in any medium, provided the original author and source are credited

Funding: (none reported)

Corresponding author: Satoshi Takagi, e-mail: satoshi.takagi@aist.go.jp

1. INTRODUCTION

It is generally recognized that the geometrical error of diamond indenters affects significantly the indicated hardness values in Rockwell hardness measurements and therefore many efforts regarding indenter verification has been made for many years. Various types of instruments have been used for the geometrical verification by many researchers, *e.g.*, the stylus-type surface profiler [1], a micro-range coordinate-measuring machine (μ CMM) [2], specific designs for spherical and conical parts of Rockwell diamond indenters in combination with interferometric optics and precise positioning mechanics [3, 4, 5], *etc.* Recently, observation techniques in small objects have been remarkably improved and 3D geometry of small objects can be obtained easier and more accurately. A 3D optical surface profiler with a white light interferometer [6], a confocal laser scanning microscope [7] and a very wide range atomic

force microscope [8] were used to observe precise 3D images of Rockwell diamond indenters. Along with those investigations, the effects of geometrical errors to hardness values are also studied by multiple regression analysis [3, 9] or a finite element analysis method [8,10]. With those backgrounds, a pilot study to investigate international metrological equivalency of Rockwell diamond indenters is now in progress under the framework of the International Committee for Weights and Measures (CIPM) [11].

The verification of the indenter geometry is important to confirm how accurately the indenter geometry follows its defined shape. It is commonly believed that a smaller geometrical error brings hardness values with higher certainty. It is, however, still difficult to improve the quality of indenters because the manufacturing technique is not much changing as the measuring techniques. For this reason, the correction of the hardness value for each indenter has been considered [12]. Yano *et al.* proposed a unique technique to estimate the bias of



Figure 1. The laser probe 3D profile measurement instrument used to measure the cross section of Rockwell diamond indenters (courtesy of Mitaka Koki, Co. Ltd.).

each indenter from the hardness value which would be realized by an ideally shaped indenter, by means of multiple regression analysis between geometric parameters of indenter and hardness [3] and it is the formal procedure to establish the national Rockwell hardness standard at the National Metrology Institute of Japan (NMIJ) until now. In order to utilize this technique, it is important for NMIJ to evaluate appropriate geometric parameters from the verification results of indenters.

In this paper the analytical method to obtain desirable geometric parameters from the measurement data of a Rockwell diamond indenter obtained with a laser probe 3D profile measurement instrument is introduced. It allows us to verify an indenter exactly compliant to the definition of CIPM and also compatible with currently used methods at NMIJ. The efficiency of the proposed analytical method was demonstrated with obtained verification results.

2. MEASUREMENT OF INDENTER GEOMETRY

The geometry of each Rockwell diamond indenter is measured with a laser probe 3D profile measurement instrument shown in Figure 1 (Model NH-3SP, Mitaka Koki, Co. Ltd., Japan) [13]. This instrument can detect the z -axis coordinate with an auto-focus mechanism with a probe laser beam through the lens during scanning of a sample on the movable sample stage. The resolution is $0.001 \mu\text{m}$ along the z -axis with a $100\times$ objective lens and $0.01 \mu\text{m}$ along the x - and y -axes. One of the advantages of this instrument is that the

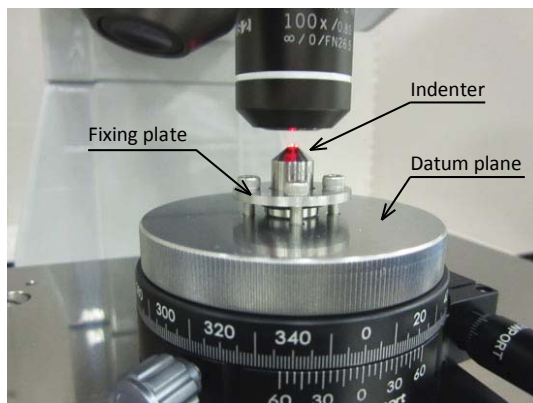


Figure 2. Setup of a Rockwell diamond indenter for the datum plane based profile measurement.

Table 1. The definition of the geometry of Rockwell diamond indenter by CIPM/CCM/WGH.

Parameters	Reference value	Start measurement	Stop measurement
Cone angle, α_m	120°	$\pm 30^\circ$	$\pm 400 \mu\text{m}$
Tip radius, R_a	$200 \mu\text{m}$	$-30^\circ \dagger$	$+30^\circ \dagger$

\dagger from the axis

measuring range is not limited in the field of view of the microscope. In addition, it has the capability to set an arbitrary coordinate system for the measurement independently from its mechanical layout. It enables us to set the datum plane for the indenter measurement. In this study, the datum plane was set on the seating face of the indenter. Due to this function, it is also possible to evaluate the tilt of the indenter axis. The setup of a Rockwell diamond indenter on the xy stage of the instrument is shown in Figure 2. In order to ensure the fitting between the datum plane and the indenter seating face, an indenter is pressed on the datum plane via an O-ring as shown in Figure 3. Profiles of a Rockwell diamond indenter are measured in eight cross sections parallel to the axis in every 22.5° . The result is graphically shown in Figure 4. In this case, the tilt of the datum plane was 0.03° and this was automatically corrected by the instrument.

3. 2D (CROSS SECTIONAL) ANALYSIS

The geometry of Rockwell diamond indenters was defined by the Working Group on hardness (WGH), Consultative Committee for Mass and Related Quantities (CCM), CIPM as Table 1 [14]. This implies that the indenter geometry should be verified by measurement of its cross section.

In order to verify an indenter according to the definition, it is important to determine the blend points between cone and sphere from the measured profile properly. The author developed an analytical method to determine the coordinate of these points with an iterative calculation. Its flowchart is

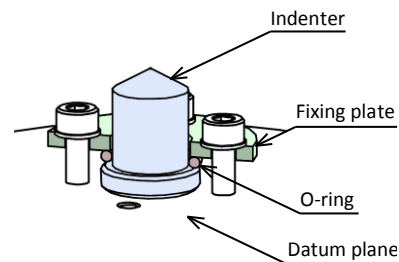


Figure 3. The detail of the sample fixture.

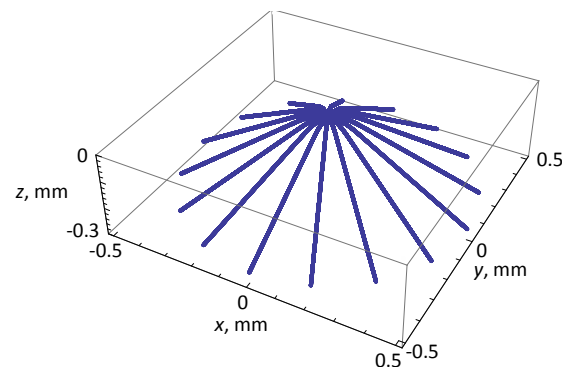


Figure 4. Measurement result of a Rockwell diamond indenter.

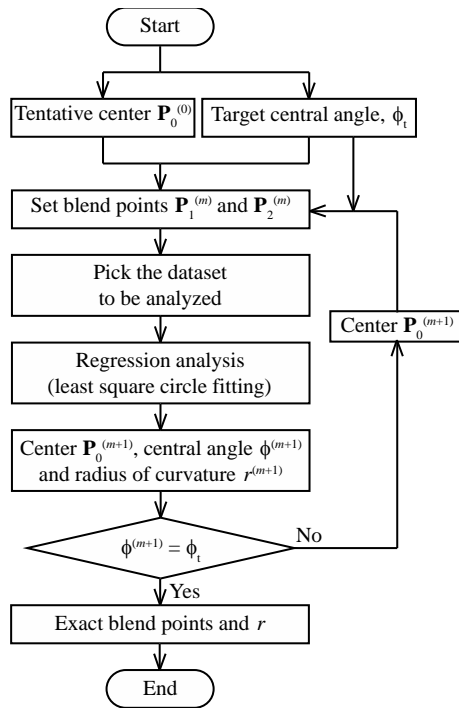


Figure 5. Flowchart for the determination of the tip radius R_s and the positions of blend points.

illustrated in Figure 5.

3.1. Extraction of the dataset to be analysed in the spherical part of indenter

For the verification of the spherical part of an indenter, the dataset of corresponding part should be extracted from the whole profile data in the central angle range between $-\phi_t/2$ ($\mathbf{P}_1^{(m)}$) and $\phi_t/2$ ($\mathbf{P}_2^{(m)}$), where $\phi_t = 60^\circ$ in the WGH/ISO compliant verification (see Figure 6). The symbol m between the parentheses represents the number of the iteration. In the beginning of the iterative calculation, the tentative centre of curvature ($\mathbf{P}_0^{(0)}$) should be determined.

3.2. Least square circle fitting

There are several methods to fit a circle to data [15]. The simplest and the most primitive way is chosen for this analysis. In order to fit the data to the equation

$$(x - a^{(m)})^2 + (z - b^{(m)})^2 = r^{(m)2}, \quad (1)$$

the following function can be taken as a measure of the fitting:

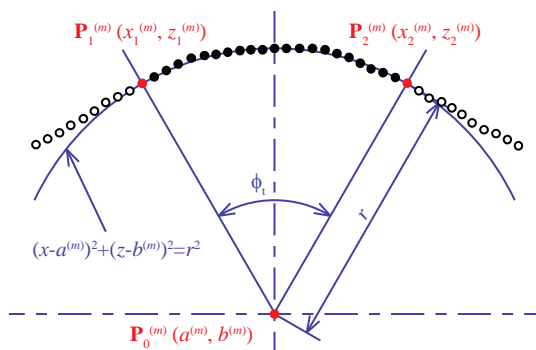


Figure 6. Extraction of the dataset of the spherical part from whole profile data corresponding to the central angle ft.

$$SS(a^{(m)}, b^{(m)}, r^{(m)}) = \sum_{i=1}^N \left(r^{(m)} - \sqrt{(x_i - a^{(m)})^2 + (z_i - b^{(m)})^2} \right)^2 \quad (2)$$

Following the least square principle, the constants $a^{(m)}$, $b^{(m)}$ and $r^{(m)}$ are determined when equation (2) is minimized.

3.3. Calculation of the central angle of the spherical part

After the least square circle fitting analysis, different points of the centre of the spherical part are obtained from the previous iteration or the initially estimated position. It brings a different central angle expressed by the following equation:

$$\phi^{(m)} = \tan^{-1} \frac{z_N^{(m)} - b^{(m)}}{x_N^{(m)} - a^{(m)}} - \tan^{-1} \frac{z_1^{(m)} - b^{(m)}}{x_1^{(m)} - a^{(m)}}. \quad (3)$$

where N is the number of data points in the selected dataset.

3.4. Iteration

If $\phi^{(m)} \neq \phi_t$, pick a different dataset according to the procedure described in 3.1 with parameters $a^{(m)}$ and $b^{(m)}$ and carry out the analysis. When $\phi^{(m+1)}$ agrees with ϕ_t within the resolution of the dataset, the best evaluation of the spherical part of an indenter is obtained.

3.5. Convergence criterion

An iterative calculation does not always bring the right answer but it works when the convergence criterion is satisfied. Let the deviation of the calculated central angle $\phi^{(m)}$ from the target angle ϕ_t be

$$F(\phi^{(m)}) \equiv \phi^{(m)} - \phi_t. \quad (4)$$

When the solution is found, equation (4) goes to zero.

As seen in equation (3), $\phi^{(m)}$ is a function with 6 parameters, i.e.:

$$\phi^{(m)} = f(x_1^{(m)}, z_1^{(m)}, x_N^{(m)}, z_N^{(m)}, a^{(m)}, b^{(m)}). \quad (5)$$

Then the convergence criterion of this iterative calculation can be written as

$$\nabla F(\phi^{(m)})^T \cdot \mathbf{d}^{(m)} < 1 \quad (6)$$

where

$$\nabla F(\phi^{(m)}) = \begin{pmatrix} \partial F(\phi^{(m)}) / \partial x_1^{(m)} \\ \partial F(\phi^{(m)}) / \partial z_1^{(m)} \\ \vdots \\ \partial F(\phi^{(m)}) / \partial b^{(m)} \end{pmatrix} \quad (7)$$

and

$$\mathbf{d}^{(m)} = \begin{pmatrix} x_1^{(m)} - x_1^{(m-1)} \\ z_1^{(m)} - z_1^{(m-1)} \\ \vdots \\ b^{(m)} - b^{(m-1)} \end{pmatrix}. \quad (8)$$

Unfortunately, the function $F(\phi^{(m)})$ is too complicated because it includes results of the least square analysis and it is not easy to show its convergence property with equations. In the analyses the author carried out, however, the iterative calculation converged in all cases. Figure 7 shows the convergence property of the iterative calculation. Four cross sections were analysed with the proposed method and in all cases the central angle $\phi^{(m)}$ converged to the target value $\phi_t = 60^\circ$ with the number of iterations between 6 and 8. It suggests empirically that the algorithm satisfies its convergence criterion.

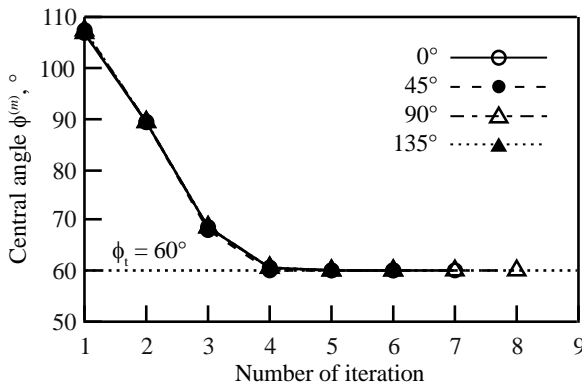


Figure 7. Convergence property of the iterative calculation.

3.6. Analysis of the conical part

Once the blend points between the sphere and cone, P_1 and P_2 , are determined, the end points of verification of the generatrices, P_3 and P_4 can be determined as points 400 μm distant from P_1 and P_2 , respectively. If the angle between the generatrices and the indenter axis are called β_1 and β_2 , the coordinates of the end points can be expressed as

$$P_3 (z_1 - 400 \mu\text{m} \cdot \cos(90^\circ - \beta_1), z_3) \quad (9)$$

and

$$P_4 (z_2 + 400 \mu\text{m} \cdot \cos(90^\circ - \beta_2), z_4). \quad (10)$$

where

$$\beta_1 \approx \beta_2 \approx \frac{\alpha_m}{2} \approx 60^\circ. \quad (11)$$

The values of $90^\circ - \beta_1$ and $90^\circ - \beta_2$ can be calculated from the slope of the linear regression of generatrices

$$z = p_1 x + q_1 \quad (12)$$

and

$$z = p_2 x + q_2 \quad (13)$$

in the respective ranges, *i.e.*, the ranges between P_1 and P_3 , and between P_2 and P_4 . In equations (9) and (10), z_3 and z_4 should be picked from the actual profile data.

The included angle of the cone α_m is calculated from the equation $\alpha_m = \beta_1 + \beta_2$.

The straightness of the generatrices can be evaluated as the deviation range from the regression lines, equations (12) and (13), in the normal direction to those lines.

4. 3D ANALYSIS

In the ISO standard [17], it is mandated that the indenter geometry shall be verified with *at least eight axial section planes, equidistant to each other*. It means that every cross section is verified independently. However, it seems to be reasonable if all measured data are verified at once as a 3D surface because the indenter geometry is actually three dimensional. In this section, a verification method by which the indenter tip is assumed as a sphere is presented.

The equation of a sphere is expressed as

$$(x - a^{(m)})^2 + (y - b^{(m)})^2 + (z - c^{(m)})^2 = r^{(m)2}. \quad (14)$$

In this case, the measure of fitting is

$$\begin{aligned} & \text{SS}(a^{(m)}, b^{(m)}, c^{(m)}, r^{(m)}) \\ &= \sum_{i=1}^N \left(r^{(m)} - \sqrt{(x_i - a^{(m)})^2 + (y_i - b^{(m)})^2 + (z_i - c^{(m)})^2} \right)^2. \end{aligned} \quad (15)$$

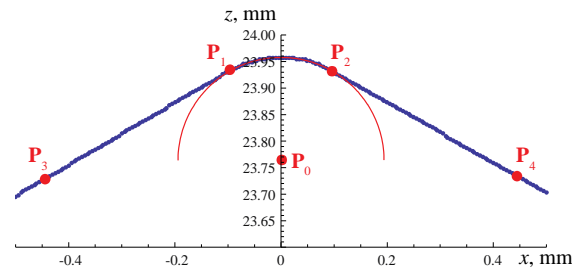


Figure 8. Graphical representation of a result of cross sectional analysis in the 0° section.

Following the same algorithm as with the 2D analysis described in the previous section, the regression sphere corresponding to the target central angle can be obtained.

When the indenter tip geometry is evaluated as a single sphere, it is necessary to verify the imperfection of the geometry in any way. One of the measures of imperfection is its *sphericity*. It can be evaluated by the deviation of measured data from the regression sphere,

$$\begin{aligned} & \delta(x_i, y_i) \\ &= \sqrt{(x_i^{(m)} - x_0^{(m)})^2 + (y_i^{(m)} - y_0^{(m)})^2 + (z_i^{(m)} - z_0^{(m)})^2} - r^{(m)} \end{aligned} \quad (16)$$

and the difference between the maximum and minimum value of $\delta(x_i, y_i)$ represents the sphericity of the indenter tip.

5. RESULTS OF THE ANALYSIS AND DISCUSSIONS

In this paper, two kinds of analytical results are shown. One is the verification compliant to the specification of WGH/ISO, based on the 2D (cross sectional) analyses. Another is 3D analysis including a compatible method to the calibration method developed and actually used in NMIJ to establish the national standard indenters.

5.1. WGH/ISO compliant verification (2D analyses)

As an example, eight cross sections of a Rockwell diamond indenter were analysed according to the procedure introduced in the previous section with the target central angle $\phi_i = 60^\circ$. The centre of curvature P_0 , the blend points P_1 and P_2 , the end points for the evaluation of generatrices P_3 and P_4 are illustrated with the fit circle on the profile data in Figure 8 for the 0° section.

The calculated average tip radius R_a and the circularity are shown in Table 2. The circularity is calculated on the basis of the minimum zone circles, *i.e.*, it is the separation of two concentric circles that just enclose the circular section of the profile. The average tip radius of eight sections is 0.19621 mm

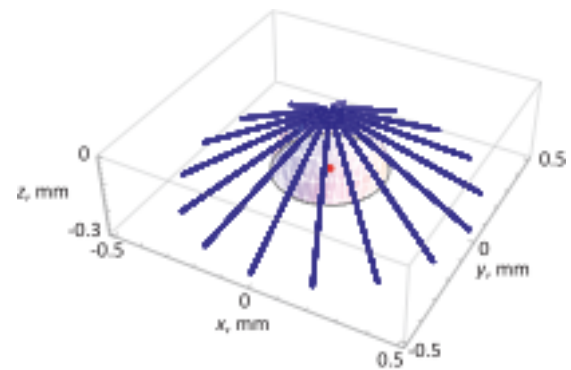


Figure 9. Graphical representation of the result of sphere fitting with target angle of 60°.

Table 2. Verification result of the spherical part of the indenter through cross sectional analysis.

Position	Tip radius R_s , mm	Circularity, mm
0°	0.19515	0.00058
22.5°	0.19621	0.00069
45°	0.19726	0.00115
67.5°	0.19602	0.00169
90°	0.19496	0.00182
112.5°	0.19659	0.00153
135°	0.19707	0.00133
157.5°	0.19640	0.00104
Average	0.19621	0.00123
Standard deviation	0.00082	—

and its standard deviation is 0.00082 mm. The circularity is between 0.00058 mm and 0.00182 mm. These results satisfy the requirement of ISO Part 3 grade specifications [17]. An apparent relationship between tip radius and its circularity is not observed in these results.

In Table 3, the analytical results for the conical part, *i.e.*, the angle between the axis and generatrices $\alpha_m/2$ (β_1, β_2), included angles of cone α_m and the straightness of generatrices are listed. The average of $\alpha_m/2$ is 59.95° whereas its standard deviation is 0.04°. Therefore, the average cone angle α_m is 119.91°. The straightness of generatrices is between 0.00032 mm and 0.00137 mm. These results also satisfy the requirement of ISO Part 3 grade requirement. An apparent relationship between angles and straightness is also not observed.

As a conclusion of the analyses, this indenter satisfies ISO Part 3 grade requirement in a completely compliant way of verification to the CIPM/CCM/WGH definition.

5.2. 3D analysis

In Figure 9, the result of sphere fitting with target angle of 60° is illustrated. The radius of the regression sphere is 0.19544 mm and the sphericity is 0.00329 mm. Comparing this result with the results in the cross sectional analyses shown in the previous subsection, the tip radius is smaller by 0.00077 mm than the average radius in the cross sectional analyses and the sphericity is greater by 0.00329 mm than the average circularity in the cross sectional analyses. The reason of these differences may be that the centres of curvature were determined independently in every cross section analysis whereas the centre of sphere is a single point in 3D analysis. In Figure 10, the contour plot of the deviation from the regression sphere of the spherical part of the indenter is illustrated. It suggests that the indenter tip is not perfectly spherical but has a complicated geometry.

In NMIJ, every standard indenter is characterized by the multiple regression analysis and has an individual correction value to determine the true hardness [3, 9]. The geometrical parameters used in this analysis are average tip radii in five different ranges set by an aperture in the microscopic measuring device and the cone angle. This aperture works to change the effective numerical aperture (NA) of the optical system. Therefore, the range under evaluation is expressed by NAs (Figure 11).

As seen in Figure 11, the NA relates to the indentation depth h_c . Therefore it can be regarded that these parameters are equivalent to the relation between the average radii of the

Table 3. Verification results of the conical part of the indenter through cross sectional analysis.

Position	Angle between the axis and generatrix, $\alpha_m/2$	Cone angle, α_m	Straightness of generatrix, mm
0°	60.01°	119.97°	0.00052
22.5°	59.93°	119.91°	0.00032
45°	59.89°	119.85°	0.00062
67.5°	59.86°	119.82°	0.00102
90°	59.90°	119.87°	0.00036
112.5°	59.98°	119.98°	0.00057
135°	59.96°	119.93°	0.00103
157.5°	59.96°	119.93°	0.00050
180°	59.96°	—	0.00042
202.5°	59.98°	—	0.00048
225°	59.97°	—	0.00040
247.5°	59.96°	—	0.00087
270°	59.97°	—	0.00111
292.5°	60.00°	—	0.00080
315°	59.98°	—	0.00137
337.5°	59.98°	—	0.00070
Average	59.95°	119.91°	0.00069
Standard deviation	0.04°	0.06°	—

indenter tip with respect to different indentation depth. The relation between NA, central angle and contact depth is calculated for the indenter being shaped exactly according to the ISO standard, and are shown in Table 4. The range for NA = 0.65 is wider than the spherical part of the ideally shaped indenter. The reason why the radius of the range beyond the blend point is included is to evaluate imperfections of the geometry around the blend point.

In order to keep the continuity between the currently used verification results and the newly introduced ones, it is useful for us to express the geometry of the spherical part of the indenter as the function of the central angle. The measuring method used in this investigation doesn't have the function to change the measuring range like the currently used instrument of NMIJ, but the same parameters can be obtained if the iterative calculation described in Section 3 is used, *i.e.*, carrying out the iterative regression analysis with the target central angle ϕ which corresponds to the NA of the currently used

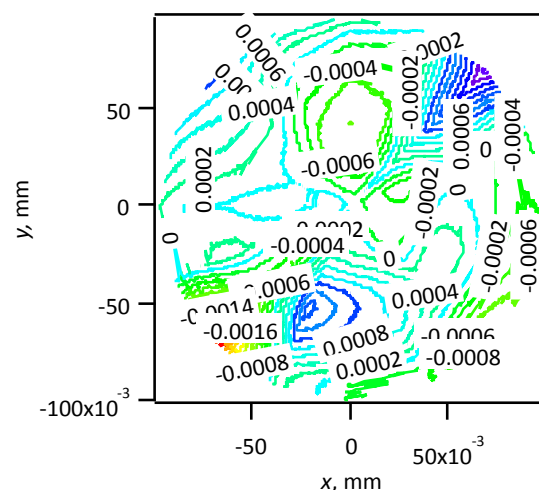


Figure 10. Deviation from the regression sphere of the spherical part of the indenter.

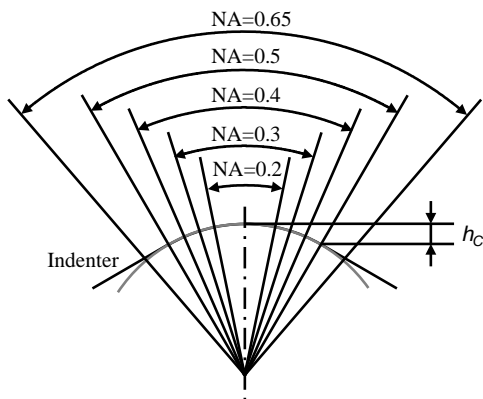


Figure 11. Evaluation of geometry of spherical part of indenter adopted by NMIJ.

verification instrument. The result of this technique is shown in Figure 12 as open dots. As seen in this chart, the average radius between $NA = 0.20$ to 0.50 , *i.e.*, the whole spherical part, is not constant for this indenter. In other words, the deviation from the definition ($R_a=200 \mu\text{m}$) depends on the indentation depth. It suggests that the deviation of hardness of this indenter from true hardness would be different for different hardness levels of the test materials.

In Figure 12, the average radii evaluated in every 5° of central angle are shown as solid dots to demonstrate the advantage of the proposed analytical method. Those values are obtained from only one measurement but it shows that the proposed method brings more information than the currently used optical method. This result describes the geometry of this indenter in more detail, *i.e.*, the radius of this indenter is almost constant in most of the range but smaller just in the vicinity of the tip.

6. CONCLUSIONS

The geometry of a Rockwell diamond indenter was measured with a laser probe 3D profile measurement instrument. The result was analysed according to the definition by CIPM/CCM/WGH and the method compatible to the one currently employed in NMIJ for the national standard

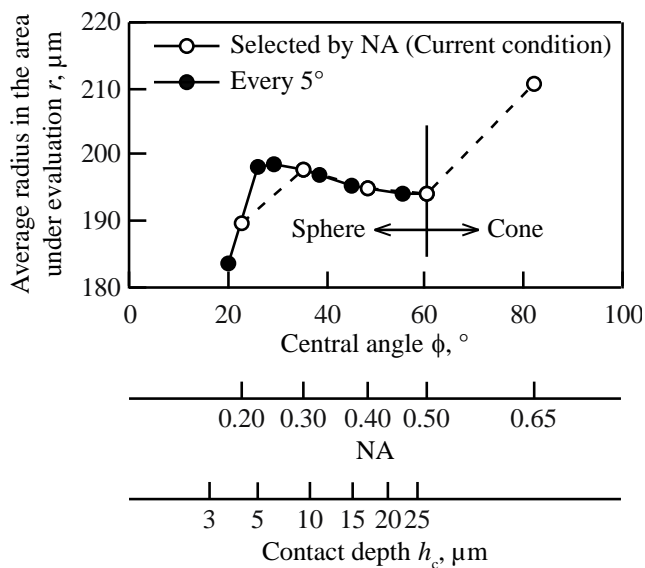


Figure 12. Average tip radius in the different evaluation area in the spherical part of indenter.

Table 4. Relation between the central angles and the contact depths of the ideally shaped indenter shown with the numerical apertures (NAs) of the optical measurement system of NMIJ.

NA	Central angle	Contact depth, mm
0.20	23.07°	0.00404
0.30	34.92°	0.00921
0.40	47.16°	0.01670
0.50	60.00°	0.02679
0.65	81.08°	0.04540†

† including the conical part of the indenter

indenters. In order to carry out those verifications, the iterative regression method is proposed to determine the desirable range for the verification. It helps us to determine the exact positions of the blend of sphere and cone or the specified range necessary for the characterization of indenters. Results of the analysis of a Rockwell diamond indenter are shown as an example for the both purposes.

The example demonstrates that the method can determine exact blend points of the cone and sphere and it enables us to verify indenters in a fully compliant way to the definition of WGH.

It is also shown that the same result with the currently used method in NMIJ can be obtained even though different principles and instruments are used for the current and newly proposed procedures. The newly proposed method suggests the capability to describe the geometry in more detail than the currently used method. It is expected that the characterization of standard indenters, *i.e.*, specific bias of each standard indenter from the true hardness value, will be carried out in better accuracy and minimizing the uncertainty of the national standard indenters.

REFERENCES

- [1] J. Song, S. Low, A. Zheng and P. Gu, "Geometrical Measurements of NIST SRM Rockwell hardness diamond Indenter", Proceedings of IMEKO 2010: TC3, TC5 and TC22 Conferences, pp. 137-140, 2010.
- [2] O. Kruger, L. Mostert, "The Use of a μCMM in the Calibration of Hardness Indenters", Proceedings of HARDIMEKO 2007, pp. 103-105, 2007.
- [3] H. Yano, H. Ishida and T. Kamoshita, "Characteristics of the Standard Rockwell Diamond Indenters and Method of Establishing Standard Indenters", Proceedings of the Round-Table Discussion on Hardness Testing, 7th IMEKO, London, 16, 1976.
- [4] T. Narumi, T. Nakamura, Y. Ichihara, Y. Saruki and J. Miyakura, "Measuring System for Micro Radius", Optomechatronic Systems III, Proceedings of the Society of Photo-Optical Instrumentation Engineers (SPIE), pp. 262-269, 2002.
- [5] A. Liguori, A. Germak, G. Gori, E. Messina, "Galindent: the reference metrological system for the verification of the geometrical characteristics of Rockwell and Vickers indenters", VDI-Berichte, vol. 1685, pp. 365-371, 2002.
- [6] Y.-L. Chen and D.-C. Su, "A method for measuring the geometrical topography of a Rockwell diamond indenter", Measurement Science and Technology, vol. 21, pp. 1-7, 2010.
- [7] A. Germak and C. Origlia, "Investigations of New Possibilities in the Calibration of Diamond Hardness Indenters Geometry", Measurement, vol. 44, pp. 351-358, 2011.
- [8] G. Dai, J. Zhao, F. Menclao, K. Herrmann and U. Brand, "Improved Methods for Accurately Calibrating the 3D

- Geometry of Rockwell Indenters”, Proceedings of IMEKO 2010: TC3, TC5 and TC22 Conferences, pp. 141-144, 2010.
- [9] S. Takagi, H. Ishida, T. Usuda, H. Kawachi and K. Hanaki, “Direct Verification and Calibration of Rockwell Diamond Indenters”, HARDIMEKO 2004, pp. 149-154, 2004.
- [10] L. Ma, S. Low, J. Zhou, J. Song and R. deWit, “Simulation and Prediction of Hardness Performance of Rockwell Diamond Indenters Using Finite-Element Analysis”, *Journal of Testing and Evaluation*, vol. 30, no. 4, pp. 265-273, 2002.
- [11] A. Germak and S. Low, Summary Report of The Consultative Committee for Mass and Related Quantities (CCM) Working Group on Hardness (WGH) 13th Meeting, 21 Sep., 2011.
- [12] D. Schwenk, K. Herrmann, G. Aggag and F. Menelao, “Investigation of a Group Standard of Rockwell Diamond Indenters”, Proceedings of HARDIMEKO 2007, pp. 106-111, 2007.
- [13] K. Miura and M. Okada, “Three-Dimensional Measurement of Wheel Surface Topography with a Laser Beam Probe”, *Advances in Abrasive Technology III*, Society of Grinding Engineers (Tokyo), pp. 303- 308, 2000.
- [14] A. Germak and S. Low, Summary Report of The Consultative Committee for Mass and Related Quantities (CCM) Working Group on Hardness (WGH) 8th Meeting, 16 and 21 Sep. 2006.
- [15] D. Umbach and K. N. Jones, “A Few Methods for Fitting Circles to Data”, *IEEE Transactions on Instrumentation and Measurement*, vol. 52, issue 6, pp. 1881-1885, 2003
- [16] ISO 6508-2: 2005, “Metallic materials — Rockwell hardness test — Part 2: Verification and calibration of testing machines (scales A, B, C, D, E, F, G, H, K, N, T)
- [17] ISO 6508-3: 2005, “Metallic materials — Rockwell hardness test — Part 3: Calibration of reference blocks (scales A, B, C, D, E, F, G, H, K, N, T)